Heritage Science

RESEARCH

Open Access

Search for new materials based on chitosan for the protection of cultural heritage

Anna Ermolyuk[1*], Darya Avdanina[1*], Adelya Khayrova[1], Sergey Lopatin[1], Kirill Shumikhin[2], Tat'yana Kolganova[1], Nikolay Simonenko[3], Alexey Lunkov[1], Valery Varlamov[1], Mikhail Shitov[2] and Alexander Zhgun[1]

Abstract

Microorganisms are a significant cause of damage to cultural heritage, including paintings. Currently, the palette of antiseptics that are used in painting has narrowed considerably. This is due to the increased demands placed on such substances. It was shown that low molecular weight chitosan (LMWC) obtained from the king crab (*Paralithodes camtschaticus*) exhibits high activity against dominant fungi-destructors of paintings in the State Tretyakov Gallery. Nevertheless, the increasing market demand for chitosan has prompted the exploration of alternative sources. Insects, notably the bioconverter black soldier fly (*Hermetia illucens*), stand out as one of the most cultivated options. This study investigates the effectiveness of chitosan, isolated from *H. illucens* by a novel method developed by authors, in inhibiting fungi that damage tempera paintings. The activity of 33 and 39 kDa chitosans from *H. illucens* is comparable to the most active chitosans previously studied from *P. camtschaticus*. However, there are characteristic differences between these compounds, as shown by the results of FTIR spectroscopy, which may affect their consumer properties when used in paint materials. Our studies suggest that LMWC from *H. illucens* is a promising material that can expand the range of antiseptics used in painting.

Keywords Chitosan, Depolymerisation, Antifungal activity, *Hermetia illucens*, Protection of cultural heritage

*Correspondence:
Anna Ermolyuk
anya_ermolyuk@mail.ru
Darya Avdanina
d.avdanina@gmail.com
Full list of author information is available at the end of the article

Graphical Abstract

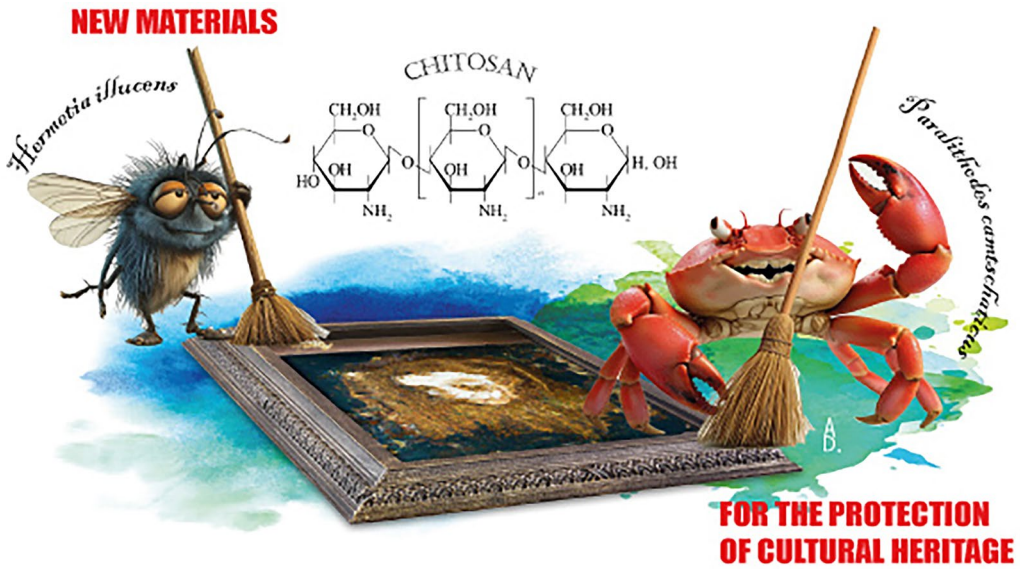

Introduction

Due to the presence of organic and inorganic components that microorganisms can use as a substrate for their activity, cultural heritage objects are often susceptible to biodegradation [1, 2]. Destructive microorganisms can cause discolouration, staining, and crumbling of materials [3]. Egg whites and yolks, which are used as substrates by destructive microorganisms, are a major cause of biodegradation in tempera paintings [4].

The rejection of conventional preparations, found to be highly toxic to restorers and museum visitors, has significantly narrowed down the list of safe antiseptics for cultural heritage objects and restorers [5–8]. Consequently, the variety of antiseptics available is restricted, leading to diminished efficacy in managing microorganisms harmful to painting materials.

In this context, chitosan emerges as a promising and ecologically sound compound for the intended purpose. Chitosan, a deacetylated form of chitin, is a widely studied natural polymer with applications in biomedicine, cosmetics, biotechnology, agriculture, and food industry (Fig. 1). Chitosan has recently been employed for the purpose of cleaning the surface of marble [9], reinforcing and fire-retardant action of paper [10], removal of hazardous pollutants from aqueous solutions [11] and protection of artworks by absorption of gaseous pollutants [12]. The most common source of chitin is crustacean waste, which has been claimed as no longer sustainable

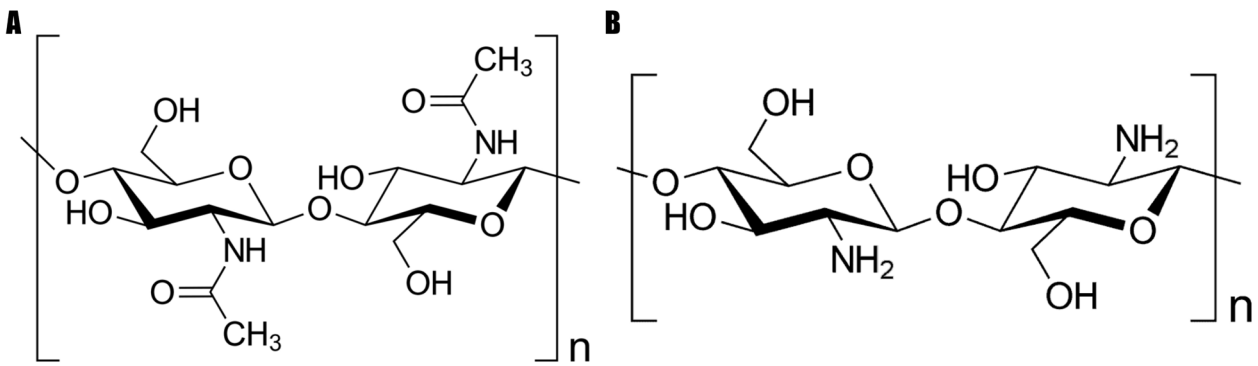

Fig. 1 Chemical structure of: **A**—chitin; **B**—chitosan

due to its dependency on environmental conditions and climate change [13]. It is also assumed that shell infection in crustaceans as well as environmental contamination add difficulties to the biopolymer production [14].

Therefore, alternative sources of chitin have been recently gaining more attention. *Hermetia illucens* or black soldier fly is considered as a promising tool to bioconvert organic waste into high-value products. An increasing number of studies aim to investigate the potential of chitosan obtained from *H. illucens* as a substitute to commercial chitosan from marine sources [15–18]. For instance, recent studies have demonstrated that low molecular weight chitosan (LMWC), isolated from *H. illucens*, exhibits improved antibacterial activity [15–17].

It has been stated that one of the main limitations of chitosan in several applications is its low solubility at neutral pH [19]. Low molecular weight fractions of chitosan result in improved solubility and biological activity and can be used in design of drug delivery systems [20]. Physical, chemical, and enzymatic methods have been described for the depolymerisatiton of chitosan [21]. Chemical delopymerisation is usually preferred in industry due to its simplicity, high yield and lower costs [22].

Low molecular weight chitosan, obtained from *Hermetia illucens*, is a promising material that can expand the range of antiseptics for painting. In this study, we examined the potential fungicidal properties of low molecular weight chitosan derived from *H. illucens* against prominent fungi-destructors found in the State Tretyakov Gallery (STG), Moscow. We compared it with chitosan obtained from the Kamchatka crab (*Paralithodes camtschaticus*), a traditional raw material previously shown effective inhibition of fungi-destructors [23].

Materials and methods

Materials

Commercial reagents from Fluka (Germany) and Sigma-Aldrich (USA) were used in this work. Commercial antiseptics used to protect paintings: benzalkonium chloride (BAC, commercial name Katamin AB) was from Neochemax, Russia; sodium pentachlorophenolate (NaPCP) from IndiaMART, India.

Hermetia illucens larvae of the fifth instar were provided by Entoprotech Ltd, Russia. 3000 g of larvae was blanched. The processed larvae went through the oilpress (RawMID, Russia) treatment to remove the majority of lipids, proteins and moisture. Then the resultant larvae were lyophilised and kept in air-tight plastic seal. The product contained approximately 6% of lipids and 7% of ash. 250 g of product was obtained (yield = 8%). High molecular weight chitosan was obtained according to the reaction scheme [15].

Obtaining of low molecular weight (LMWC) chitosan

Chitin extraction

Demineralisation: 1000 mL of 1% HCl was added to 100 g of the obtained material and stirred at 20 °C for 2 h, according [24]. The solid residue was separated through glass filter. It was washed with distilled water to neutral pH and lyophilised afterwards. 49.2 g of product was obtained (yield = 49%). Dried demineralised matter was sieved (pore diameter = 2 mm) and weighed. Product yield was equal to 45%.

Deproteinisation and defatting: 320 mL of 30% (w/w) NaOH was added to 24 g of demineralised biomass, left at room temperature for 30 min, then transferred to 100 °C water bath and kept for 2 h with occasional stirring, according [25]. Chitin was separated through glass filter, washed with distilled water until neutral pH and lyophilised. 4.8 g of product was obtained (yield = 20%).

Chitosan preparation

Deacetylation: the deacetylation step was performed by using 320 mL of 50% (w/w) NaOH, according [26]. The alkaline solution was added to 8.0 g of chitin and left at room temperature for 30 min. The suspension was warmed in 100 °C water bath for 2 h with occasional stirring. The suspension was cooled, washed until neutral pH, and lyophilised. 6.5 g of chitosan was obtained (yield = 81%).

Purification: 6.5 g of chitosan was dissolved in 650 mL of 1% CH_3COOH, according [15]. The solution was filtered through glass filter. 1 M NaOH was then added until pH of 10 was achieved. The solution was dialysed in Spectra/Por Dialysis Tubular Membrane MWCO:10,000 (Spectrum Laboratories Inc., USA) and lyophilised. 6.2 g of chitosan was obtained (yield = 95%). Weight-average molecular weight (M_w) = 570 kDa, degree of deacetylation (DDA) = 91%. The precipitate was collected, dried, and weighed. 0.26 g of precipitate was obtained (yield = 4%).

Commercial crab chitosan *Paralithodes camtschaticus* (Bioprogress LLC, Russia) was used as a comparison. M_w = 1040 kDa, DDA = 85%.

Acidic depolymerisation of chitosans

Acid hydrolysis of commercial crab chitosan (M_w 1040 kDa, DDA 85%) and of *H. illucens* chitosan (M_w 570 kDa, DDA 91%) was carried out according to the patented method [27]. 20 mL of nitric acid solutions with five concentration ranges (3.3, 6.6, 9.9, 13.1 and 16.4%) were added to 0.9 g of chitosan obtained from *H. illucens* larvae (M_w 570 kDa, DDA 91%). The reaction mass was stirred for 7 h at 70 °C, and the mixture was left overnight at room temperature. The formed precipitate was

collected by filtration and suspended in 40 mL of distilled water. The suspension was then heated in a water bath until complete dissolution (70–80 °C) and filtered to remove mechanical impurities. Chitosan was precipitated from solution using 5% (w/v) NaOH. The chitosan suspension was then dialysed in Spectra/Por Dialysis Tubular Membrane MWCO:14,000 (Spectrum Laboratories Inc., USA) and freeze dried. 0.45, 0.46, 0.55, 0.56 and 0.54 g (yields = 50, 51, 61, 63 and 60%) of low molecular weight chitosans were obtained for 3.3, 6.6, 9.9, 13.1 and 16.4% nitric acid concentrations respectively. M_w and DDA of the obtained samples were determined.

Characterisation of chitosan

Determination of the degree of deacetylation (DDA)

The degree of deacetylation of chitosan samples was measured by titration method using a Hanna Hi 8733 (Hanna Instruments, Romania) conductometer. At first, 0.1 g of chitosan was weighed and dissolved in 5 mL 0.1 N HCl at room temperature. Distilled water (25 mL) was added, and the chitosan solution was then titrated against 0.1 M NaOH solution. A titration curve of pH values vs. NaOH titration volume was generated. DDA was calculated according to ref. [28].

Gel permeation chromatography (GPC)

GPC was performed to determine the weight-average (M_w), number-average (M_n) molecular weights, molecular weight of the highest peak (M_p) and polydispersity indices ($PDI = M_w/M_n$) of chitosan samples by the method described by Lopatin et al. [29]. The GPC apparatus S 2100 (Sykam, Germany) comprised K-5004 degasser (Knauer, Germany), Jet Stream + column thermostat (Knauer, Germany), RI Detector K-2301 reflectometric detector (Knauer, Germany) and PSS NOVEMA Max analytical 1000 A column (PSS, Germany). Pullulans (M_w = 342, 1260, 6600, 9900, 23,000, 48,800, 113,000, 200,000, 348,000 и 805,000 Da) (PSS, Germany) were used as calibration standards. A buffer solution of 0.1 M HAc/NH_4Ac pH = 4.5, containing 0,2 M NaCl was evaluated a rate of 1. 0 mL/min. Characteristic values for chitosans were obtained using the computer program MultyCrom GPC *v*. 1.6 (Ampersand, Russia).

Fourier transform infrared spectroscopy (FTIR)

FTIR analysis was carried out with samples of chitosan from *H. illucens* (M_w = 570 kDa) and commercial crab chitosan (M_w = 1040 kDa) by using an IRAffinity-1 instrument (Shimadzu, Japan), in the range of 4000–400 cm^{-1}. Spectra were processed and analysed with the OMNIC software (Thermo Fisher Scientific, Waltham, MA, USA), as described previously [30].

Characterisation of fungal strains

Fungal strains used in this work

All strains used in the work were isolated from the exhibits and surfaces of the halls of Painting of Ancient Rus (56, 57 and 61) or in the Storage Fund of the main historical building of the State Tretyakov Gallery (10 Lavrushinsky per., Moscow) [4]. Twelve strains of filamentous fungi, previously isolated in the halls of Ancient Russian painting (No. 56, 57 and 61) or in the Storage Fund, both located in the State Tretyakov Gallery (10 Lavrushinsky per., Moscow, Russia) [4] were used as test cultures to determine the antimycotic activity of studied compounds. *Aspergillus versicolor* STG-25G (SRX7729174; MK260015.1), *Mucor circinelloides* STG-30 (SRX7729212; MK260195.1) and *Ulocladium* sp. AAZ-2020a STG-36 (MW590700.1; SRX7729176) were isolated from the icon "the Church Militant" (dated 1550 s). *Cladosporium halotolerans* STG-52B (SRX7729178; MK258720.1) was isolated from a bust fragment of the statue "Holy Great Martyr George the Victorious" (1464, Lime Stone, tempera). *Aspergillus creber* STG-57 (SRX7729151; MK266993.1) was isolated from the icon "Holy Great Martyr Demetrius of Thessaloniki" (dated sixteenth century). *Aspergillus versicolor* STG-86 (SRX7729182; MK262781.1), *Aspergillus creber* STG-93W (SRX7729186; MW575292.1), *Cladosporium parahalotolerans* STG-93B (SRX7729188; MK262909.1), *Simplicillium lamellicola* STG-96 (SRX7729192; MK262921.1) were isolated from the surfaces of hall №61. *Microascus paisii* STG-103 (SRX7729190; MW591474.1) was isolated from the hall №57. *Aspergillus protuberus* STG-106 (SRX7729192; MK268342.1) was isolated from the hall №56. *Penicillium chrysogenum* STG-117 (MW556011.1) was isolated from the surface of the icon "Prophet Solomon" (dated 1731).

Quantification of the inhibition of fungal growth

Filamentous fungi were cultured on slanted agarised Czapek-Dox medium (CDA) (g/L): sucrose—30; $NaNO_3$—2; K_2HPO_4—1; $MgSO_4 \times 7H_2O$—0.5; KCl—0.5; $FeSO_4 \times 7H_2O$—0.01; agar—20; pH 7.1. The antifungal activity of chitosans against colonies of filamentous fungi was determined using the drop and dilution method, as described previously with some modifications [31, 32]. A stock solution of LMWC (30 mg/mL) were dissolved in 0.1 M acetic acid, dialysed against distilled water and sterilised at 121 °C for 20 min. Cells of test cultures were harvested from agar slants and diluted with 0.9% NaCl solution to OD_{600} = 0,03; 3 µL were inoculated onto Petri dishes with CDA containing 1 mg/mL chitosan (25 and 45 kDa from *P. camtschaticus*; 33, 39, 53, 88 kDa

from *H. illucens*), or control antiseptics (0.1 mM BAC, 0.2 mM NaPCP), or without additions (control). Incubation was performed at 26 °C for 41 days. The antifungal activity was quantified as the percentage inhibition of growth of filamentous fungi colonies on CDA medium with added chitosans relative to growth on control medium, as earlier described [33, 34]. Fungal growth inhibition (FGI) was determined by the following formula:

$$FGI\,\% = [(Dc-Dt)/Dc] \times 100 \quad (1)$$

where D_c and D_t are diameters of the control and experimental colonies, respectively. The data recorded were measured in triplicate.

Scanning electron microscopy (SEM)

Microstructural features of the samples of filamentous fungi were examined by scanning electron microscopy using a Carl Zeiss NVision-40 microscope. For this purpose, representative samples were selected, which were further fixed on an aluminum objective table using conductive carbon tape. Thus, mounted samples were placed in the vacuum chamber of the microscope and air was evacuated from it until the working pressure reached about $5.5–10^{-6}$ mbar. An Everhart–Thornley secondary electron detector with a focal length of about 3.3 mm was used for the study of the materials surface. In order to minimise the impact of the electron beam on the samples structure, their surface was scanned at a sufficiently low accelerating voltage (1 kV). Due to the relatively low electrical conductivity of the specimens under study, the magnification, as a rule, was limited to the range of 250–15000 times.

Results and discussion

Obtaining chitin and chitosan

The scheme for obtaining chitin from the larvae of *H. illucens* is standard and includes demineralisation and deproteinisation steps. The demineralised biomass was sieved and divided into different fractions—more than 5 mm, 2–5 mm, and less than 2 mm. Each fraction was separately deproteinised, and the amounts of chitin were determined: the values were 30, 14 and 2%, respectively. This indicates negligible content of chitin-containing residue in the smallest fraction, which was not subjected to further processing due to economic inexpediency but can further be used as a feed additive.

Chitin was subsequently deacetylated to chitosan. After carrying out demineralisation, deproteination and deacetylation steps, some of the impurities were still present in the final product. The resulting material contained approximately 4% of the fraction insoluble in acetic acid. Presumably, this indicates the presence of 'cuticulin', a substance occurring in the exocuticle and epicuticle [35].

The chitosan obtained in this way requires additional purification by reprecipitation from a solution in acetic acid. The resulting chitosan was characterised by HPLC. M_w was 570 kDa and PDI—1.32. DDA of chitosan was calculated as 91% using the method of conductometric titration.

Acidic depolymerisation of chitosan

Figure 2 shows the dynamics of acidic hydrolysis of chitosans obtained from *H. illucens* larvae.

Low molecular weight chitosans were prepared by using nitric acid of various concentrations—3.3, 6.6, 9.9, 13.1 and 16.4%. As the acid concentration increased, degree of deacetylation of obtained chitosan also increased: 92, 95, 97, 97, and 98%, respectively. The drop

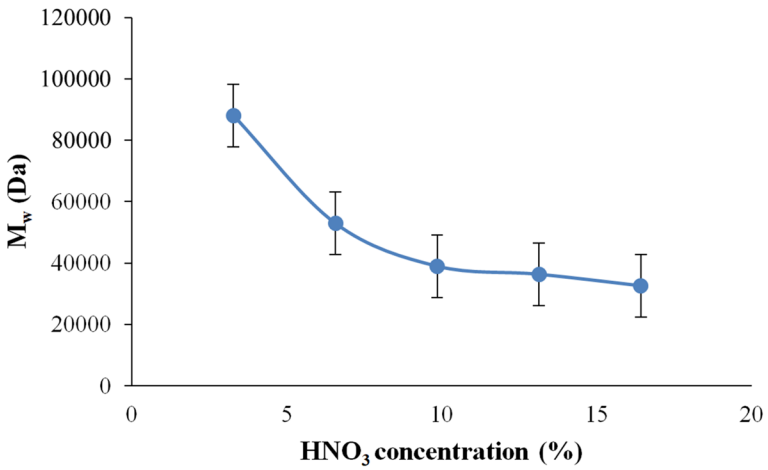

Fig. 2 Kinetics of changes in molecular weight of chitosan from *H. illucens* larvae during acidic hydrolysis

of molecular weight values was initially observed with increasing nitric acid concentration, however, reached plateau and did not fall below 33 kDa.

Using acidic hydrolysis low molecular weight chitosans (33–88 kDa) can be obtained and further used for studying their biological activity (Table 1). The purity of initial chitosan samples was confirmed by FTIR (Fig. 2) analyses.

FTIR analyses of insect chitosan and crab chitosan

To clarify the structural characteristics of chitosan, FTIR spectral analysis of *H. illucens* chitosan and *P. camtschaticus* chitosan was performed in the frequency region of 4000–400 cm^{-1} (Fig. 3).

Key IR bands at 3435, 2918, and 2881 cm^{-1} were identified in both products, corresponding to stretching vibrations of OH, NH, and CH bonds, respectively. Additional bands near 1656 and 1576 cm^{-1}, denoting amide I and II vibrations in chitosan, were observed, with the former exhibiting a contribution from the scissoring vibration of water $\delta(H_2O)$. The FTIR spectra revealed weak amide bands, confirming the high deacetylation of these products. The absence of the band at ~ 1540 cm^{-1}, typical for proteins, further affirmed effective deproteinisation. Bands at 1418 and 1380 cm^{-1} originated from bending vibrations of CH_2 and CH_3 groups $\delta(CH_2)$, $\delta_{as}(CH_3)$, and $\delta_s(CH_3)$, respectively, consistent with previous studies [36, 37]. The band at 1151 cm^{-1}, indicative of polysaccharides, was assigned to COC stretching vibrations at glycosidic bonds. Intense bands at 1083 and 1034 cm^{-1} were associated with CO stretching in pyranoid rings.

Despite minor differences in absorption spectra, the characteristic peaks of *H. illucens* chitosan closely resembled those of *P. camtschaticus* chitosan, with enhanced intensities in most absorption peaks. This affirmed their structural similarity through spectral analysis.

To assess the quantitative content of certain functional groups in chitosan, a comparison was made in relative units. The absorption intensity of the studied absorption band was compared with the intensity of band 3435 cm^{-1}

Table 1 The physicochemical characteristics of crab and insect chitosan samples

Sample	Abbreviation	M_w, kDa	M_n, kDa	M_p, kDa	PDI	DDA, %
1	88 h	88	39	63	2.24	91.8
2	53 h	53	27	36	1.99	94.8
3	39 h	39	17	24	2.31	96.7
5	33 h	33	14	23	2.32	97.9
6	45cr	45	16	22	2.99	85.4
7	25cr	25	14	15	1.81	88.6

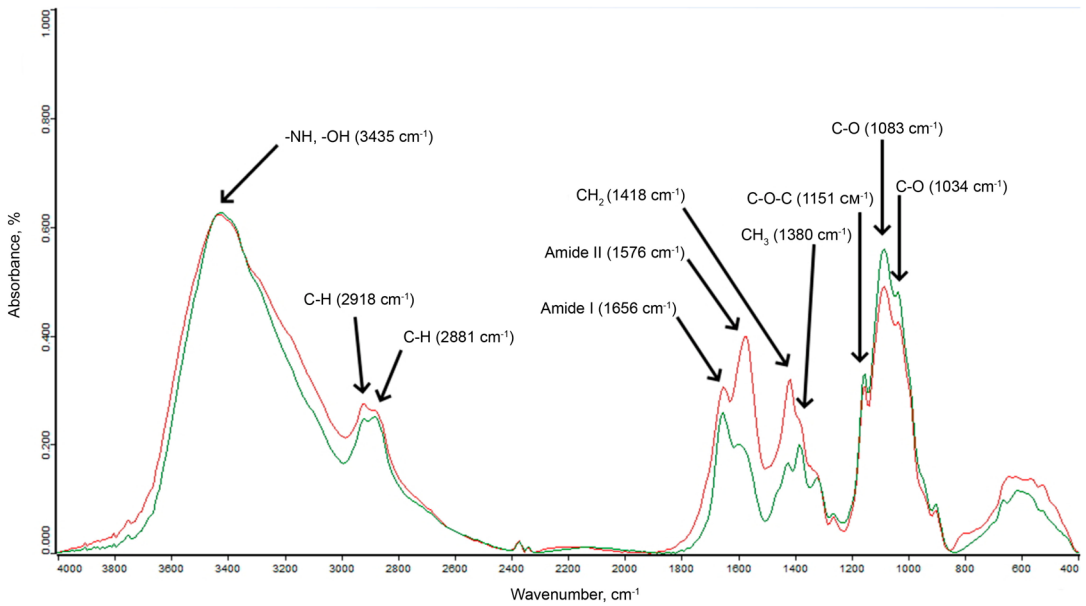

Fig. 3 Comparison of FTIR spectra of chitosan from *H. illucens* (red) and chitosan from *P. camtschaticus* (green)

(NH, OH) according to the following principle—the intensity of the studied band was divided by the intensity of the band with maximum absorption (OH, NH) and multiplied by 100 to show the percentage. This method was used for relative comparison of the intensity of chitosan bands from different raw materials (Table 2).

While common functional groups were identified in both chitosan varieties, the spectrum of *H. illucens* chitosan exhibited notably more intense bands in the N–H bond (1570 cm^{-1}, amides, proteins), CH_2 (1415 cm^{-1}), and CH_3 (1380 cm^{-1}) functional groups compared to chitosan from *P. camtschaticus*. This suggests that *H. illucens* chitosan may have slightly longer aliphatic hydrocarbon chains, indicating potential variations in the chemical extraction method or the distinct species involved. Differences may arise from impurities like melanin or other contaminants, potentially forming complexes with chitosan and influencing its chemical environment, leading to alterations in vibrational frequencies and peak shifts.

Antifungal activity

The study investigated the fungicidal activity of chitosans obtained from *H. illucens* and *P. camtschaticus* on CDA medium with two standard antiseptics and a control (no additives) against 12 filamentous fungi previously isolated in STG [4]. The fungi belonged to the following genera: *Aspergillus*, *Cladosporium*, *Simplicillium*, *Microascus*, *Ulocladium*, *Penicillium* and *Mucor*. These fungi have been intensively studied recently, both from the point of view of the possibility of using their metabolic potential for the needs of biotechnology [38], and with the aim of creating targeted antiseptics against them with a broad spectrum of action [39–41]. However, the influence of cultivation conditions on the characteristic micromorphology of these fungi has not been previously studied. And this is important, since antiseptics can have different effects on different morphological forms of fungi. In this regard, in the current study at the first stage, the micromorphology of fungi from STG, cultivated on Czapek-Dox agar medium, was studied by scanning electron microscopy (Fig. 4). It turned out that the micromorphology of fungi does not change compared to their characteristic structure when growing on painting materials. Thus, we have shown for the first time that these cultivation conditions are suitable for studying their sensitivity to antiseptics.

We then determined the antifungal activity of the studied compounds. It was quantified as the percentage inhibition of growth of filamentous fungi colonies on CDA medium with added chitosans relative to growth on control medium. Inhibition dynamics were tested using 1 mg/mL chitosans, 0.1 mM benzalkonium chloride (BAC), and 0.2 mM sodium pentachlorophenolate (NaPCP). Results were recorded every 3 days after inoculation. Figure 5 demonstrates the characteristic growth of these STG-strains after 14 days of cultivation. The cultures were incubated at 26 °C for 41 days.

In our experiment there was an opposite tendency—in the series 33–39–53–88 kDa, chitosans with the lowest M_w showed the highest inhibition efficiency, after 39 kDa the inhibitory activity was lower (Figs. 6, 7). All variants of the tested chitosans and standard antiseptics completely inhibited members of the genera *Simplicillium* and *Microascus* (Fig. 6). Chitosans from *H. illucens* and *P. camtschaticus* demonstrated high antifungal activity (100%) against *Cladosporium* species compared to BAC, whose activity decreased from 100 to 30% after 41 days of incubation. Chitosans with molecular weight 33 and 39 kDa from *H. illucens* completely inhibited almost all representatives of the *Aspergillus* genus

Table 2 Comparison of characteristic peaks from the FTIR spectra of *H. illucens* chitosan and *P. camtschaticus* chitosan

Absorption band	Chitosan from *H. illucens*		Chitosan from *P. camtschaticus*	
	Absolute absorption value, %	Comparative value	Absolute absorption value, %	Comparative value
OH, NH (3435 cm^{-1})	55.15 ± 0.90	–	62.85 ± 0.65	–
C-H (2918 cm^{-1})	24.58 ± 1.42	44.5 ± 2.32	24.36 ± 0.80	38.7 ± 1.70
C-H (2881 cm^{-1})	23.29 ± 1.10	42.2 ± 2.00	25.22 ± 0.75	40.1 ± 1.65
Amide I (1656 cm^{-1})	27.36 ± 0.61	49.6 ± 1.51	26.07 ± 0.45	41.4 ± 1.35
Amide II (1576 cm^{-1})	**35.48[a] ± 0.93**	**64.3 ± 1.83**	**20.09 ± 0.65**	**31.9 ± 1.55**
CH_2 (1418 cm^{-1})	**29.43 ± 0.49**	**53.3 ± 1.39**	**16.88 ± 0.31**	**26.8 ± 1.21**
CH_3 (1380 cm^{-1})	**22.80 ± 0.75**	**41.3 ± 1.65**	**19.87 ± 0.40**	**31.6 ± 1.30**
C–O–C (1151 cm^{-1})	**27.00 ± 1.50**	**48.9 ± 2.40**	**33.34 ± 0.72**	**53 ± 1.62**
C–O (1083 cm^{-1})	**43.61 ± 3.57**	**79 ± 4.47**	**56.22 ± 2.20**	**89.4 ± 3.10**
C–O (1034 cm^{-1})	38.41 ± 2.85	69.6 ± 3.75	48.31 ± 1.67	76.8 ± 2.57

[a] The values of peaks that have significant differences for chitosans obtained from *H. illucens* and *P. camtschaticus* are highlighted in bold

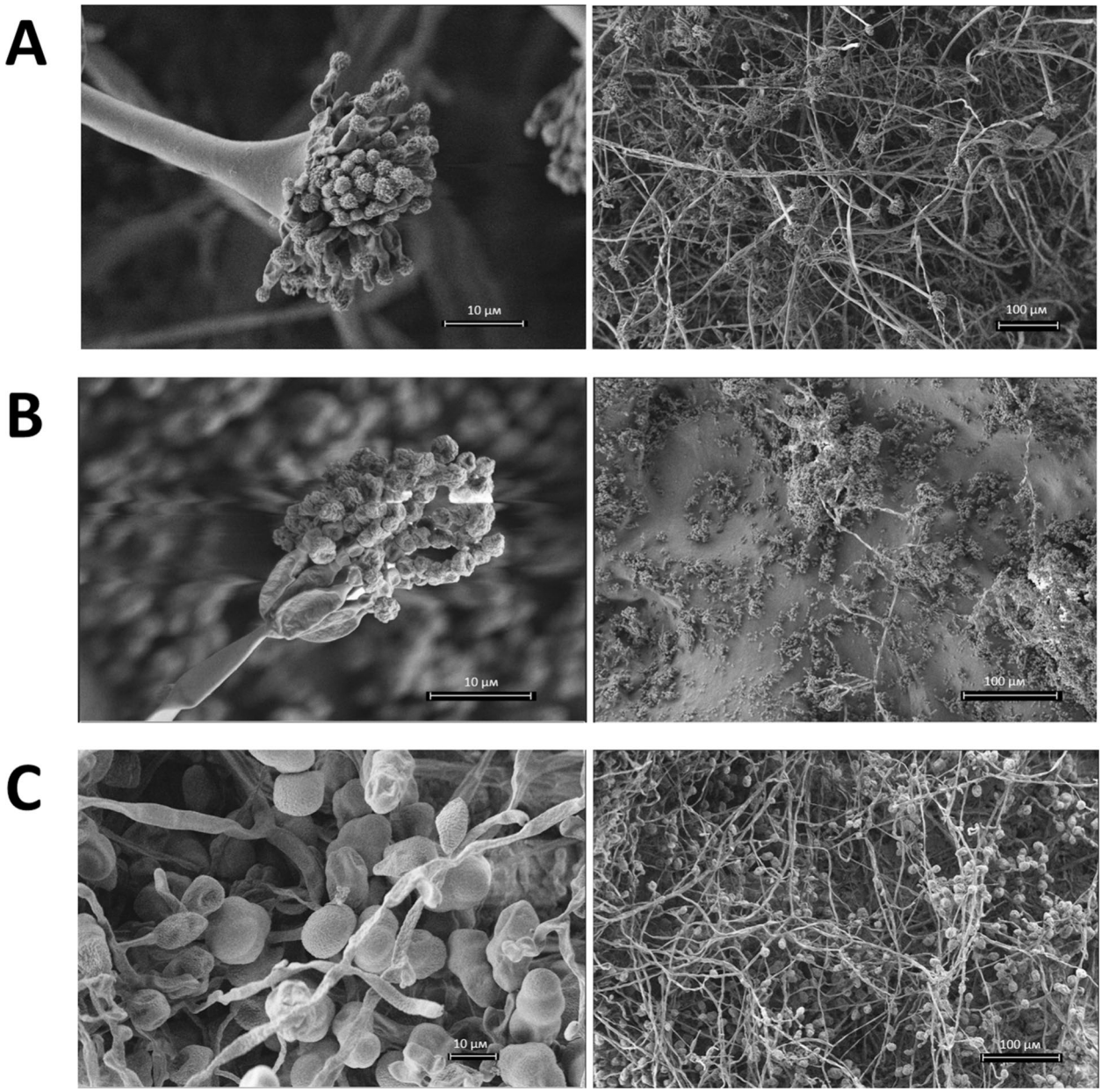

Fig. 4 Scanning Electron Microscopy of STG-strains: **A**—*Aspergillus versicolor* STG-86; **B**—*Penicillium chrysogenum* STG-117; **C**—*Ulocladium* sp. AAZ-2020a STG-36

during the whole incubation period, but the growth inhibition of *A. versicolor* (STG-86) was present during the first 10 days of incubation, then gradually decreased and reached 20% at the end of incubation (Fig. 7). Chitosans with M_w 53 and 88 kDa also inhibited representatives of this genus, in particular strains *Aspergillus creber* (STG-93W) and *A. protuberus* (STG-106); the inhibitory effect of other representatives decreased with time (up to 25–70%). Chitosans from *H. illucens* with M_w 33–53 kDa completely inhibited *Ulocladium* sp. AAZ-2020a (STG-36), while the toxic effect of chitosan with M_w 88 kDa decreased from 98 to 65% over time.

It is important to note that the growth inhibition of *P. chrysogenum* (STG-117) and *M. circinelloides* (STG-30) was less than 70% at the beginning of the incubation period and almost no inhibition was observed after 20 days of cultivation (Figs. 6, 7). Only when NaPCP was added to the medium throughout cultivation, their complete inhibition was recorded.

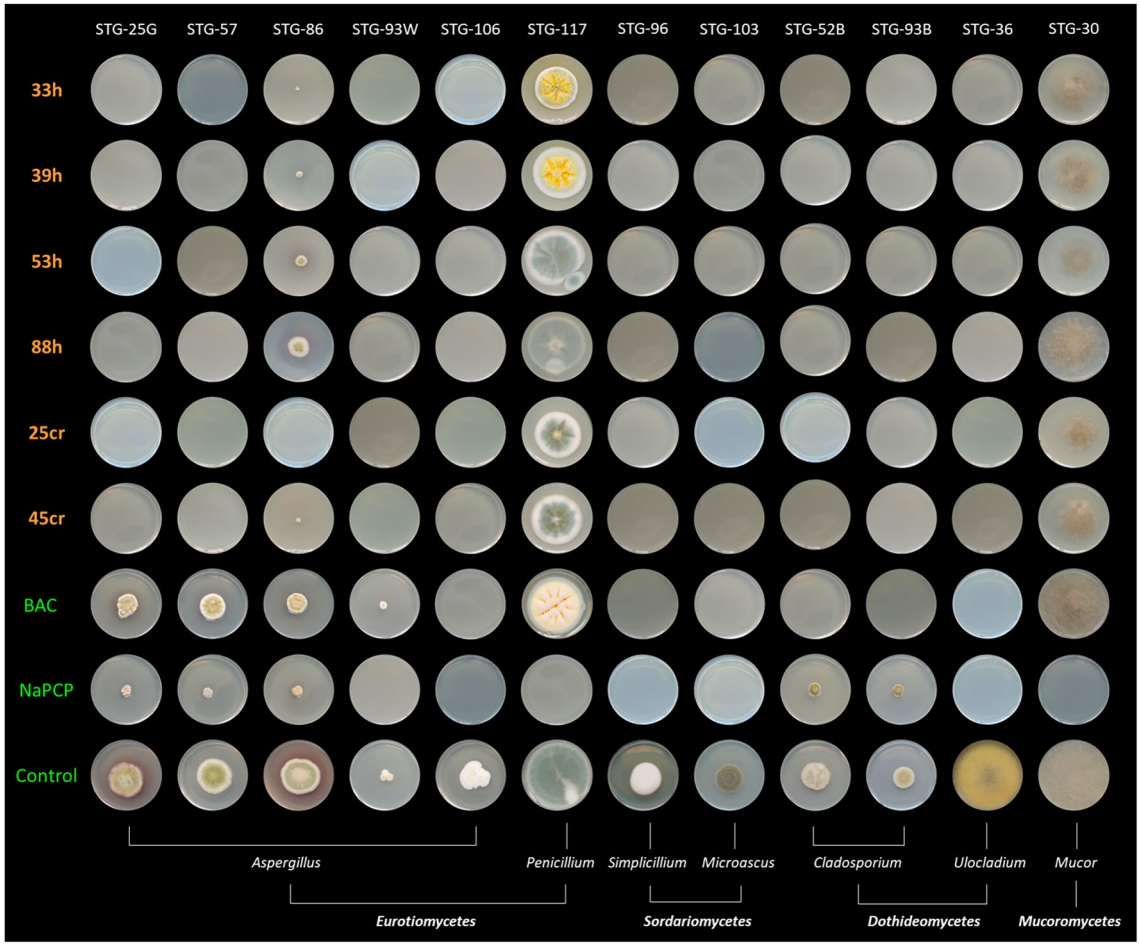

Fig. 5 The phenotype of fungi strains on CDA medium, supplemented with 1 mg/mL chitosans, 0.1 mM BAC, 0.2 mM NaPCP and without them (control). Petri dishes were captured in 14 days after inoculation

Chitosans from *P. camtschaticus* showed similarly high results as in ref. [23] work—complete growth inhibition of most strains except for *A. versicolor* (STG-86), *P. chrysogenum* (STG-117) and *Mucor circinelloides* (STG-30). However, it is noteworthy that crab chitosan with MM 25 kDa showed the highest antifungal activity against *A. versicolor* STG-86, completely inhibiting the strain during the first 14 days of incubation.

A characteristic change in micromorphology of *P. chrysogenum* STG-117, expressed as a change in pigment colouration, was induced by the addition of black soldier fly chitosan, not by chitosan from crab (Fig. 8). The main pigments in *P. chrysogenum* are sorbicillin and chrysogine, which can be synthesised in response to several stimulus and give the strain growing on agar medium a characteristic greenish-yellow hue [42]. The phenotypic difference of *P. chrysogenum* STG-117 growing on agar medium supplemented with chitosans from various sources clearly demonstrates their differences at the molecular level, leading to different effects on the secondary metabolism of the mold.

The level of inhibition at 9, 21 and 41 days for all strains tested is shown in Fig. 9. The chitosans with M_w 33 and 39 kDa from black soldier fly and 25 and 45 kDa from crab were the most active compounds, outperforming the standard antiseptic NaPCP in terms of inhibition activity. BAC and chitosans from black soldier fly with M_w 53 and 88 kDa showed the lowest activity. The graph illustrates that chitosans from *H. illucens* with MW 33 and 39 kDa and from *P. camtschaticus* with M_w 25 and 45 kDa can act as alternative antiseptics against filamentous fungi.

Chitosans' antifungal activity is related to their interaction with fungal cell walls and membranes [43]. However, the inhibition efficiency depends on the systematic group of the fungus. The lipid composition of the membranes is the main factor known to influence the efficacy of chitosan against filamentous fungi [44]. Filamentous fungi with a high content

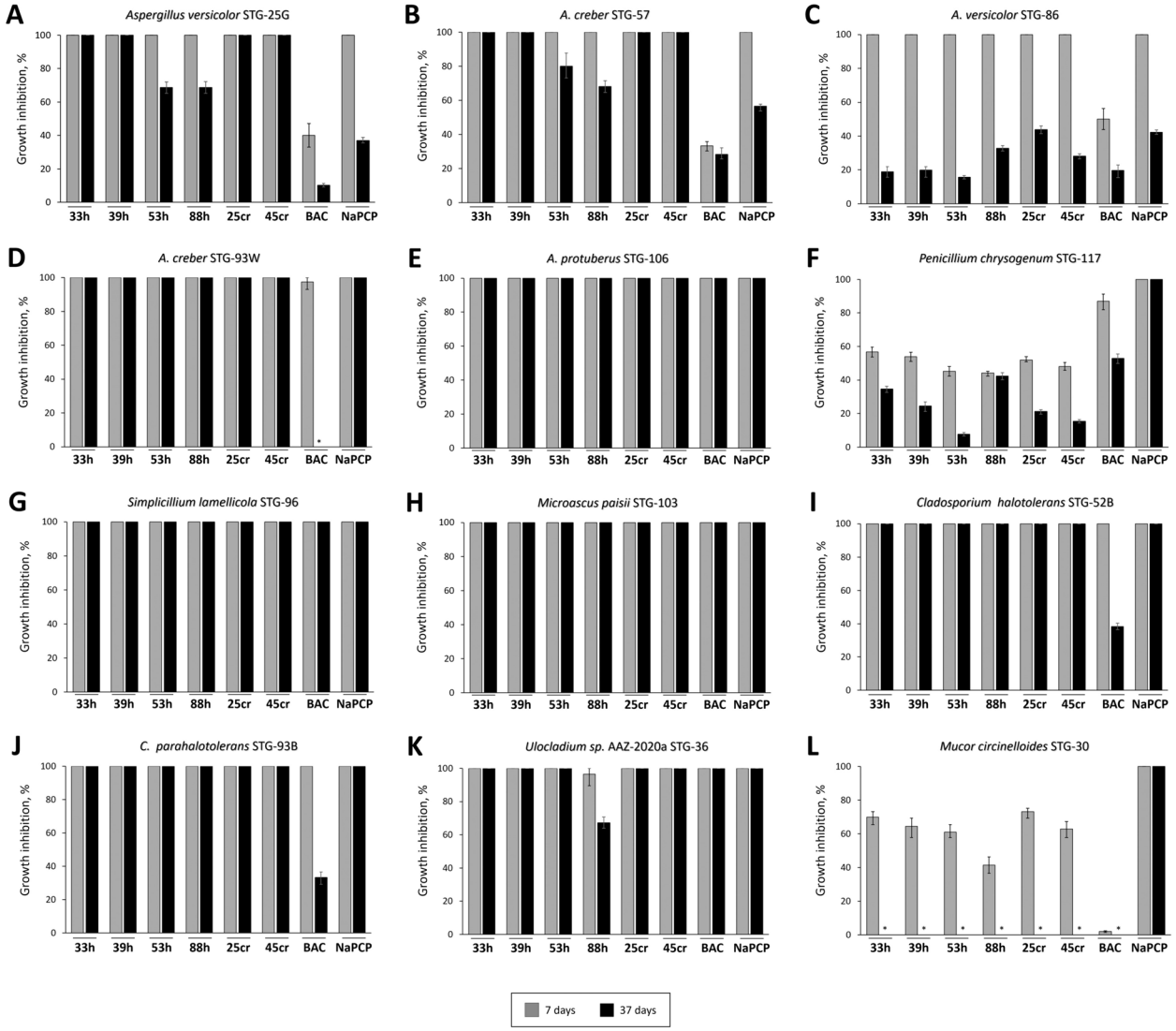

Fig. 6 Growth inhibition (%) of STG-strains on CDA with added 1 mg/mL chitosans, or 0.1 mM BAC, or 0.2 mM NaPCP. Data were obtained at 7 and 37 days after inoculation. Symbol * means "not detected"

of polyunsaturated fatty acids, such as linoleic acid, are more sensitive to chitosan. Conversely, fungi with a high content of saturated acids in the membrane are resistant to the action of chitosan. Previous studies have shown that chitosan's positive amino groups interact with the negative charges of plasma membrane phospholipids, which may lead to changes in plasma membrane permeability [45, 46]. The study [47] demonstrated that chitosan induces necrotic cell death and can penetrate the cell membrane during the early stages of fungal development without causing visible membrane disruption. This leads to a significant reduction in intracellular substance content and severe damage to the membrane structure.

It was earlier reported [48] that the biological activity of chitosan increases with a higher DDA. However, contradictory data exists regarding the relationship between antifungal activity and chitosan M_w. Some studies [49, 50] have suggested a decrease in biocidal activity with an increase in chitosan M_w, while others have found higher activity in high molecular weight chitosans compared to low molecular weight ones [51–53].

The conflicting results in the activity-M_w relationship are attributed to variations in characteristics of molecular weight, DDA, and preparation methods among chitosan samples used by different investigators [54, 55]. The reported differences in biological effects could also stem from the presence of various types and quantities of

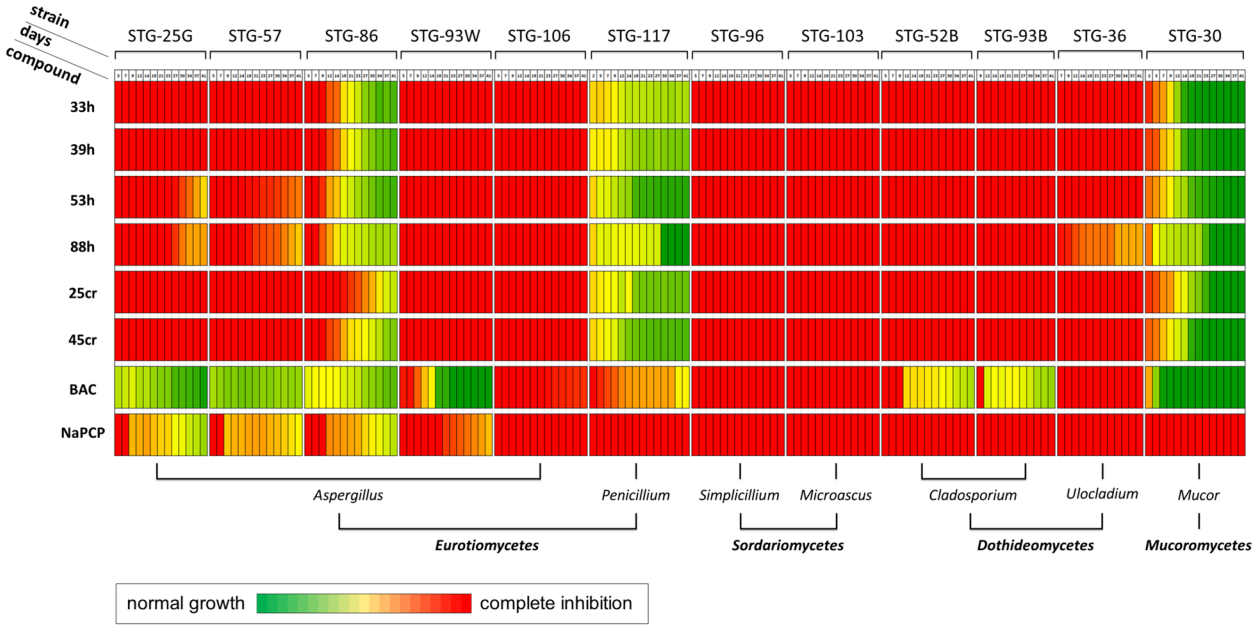

Fig. 7 Dynamics of growth inhibition of STG-strains on CDA medium with 1 mg/mL chitosans, or 0.1 mM BAC, or 0.2 mM NaPCP after 2, 5, 7, 9, 12, 12, 14, 19, 21, 24, 27, 30, 34, 37 and 41 days after inoculation

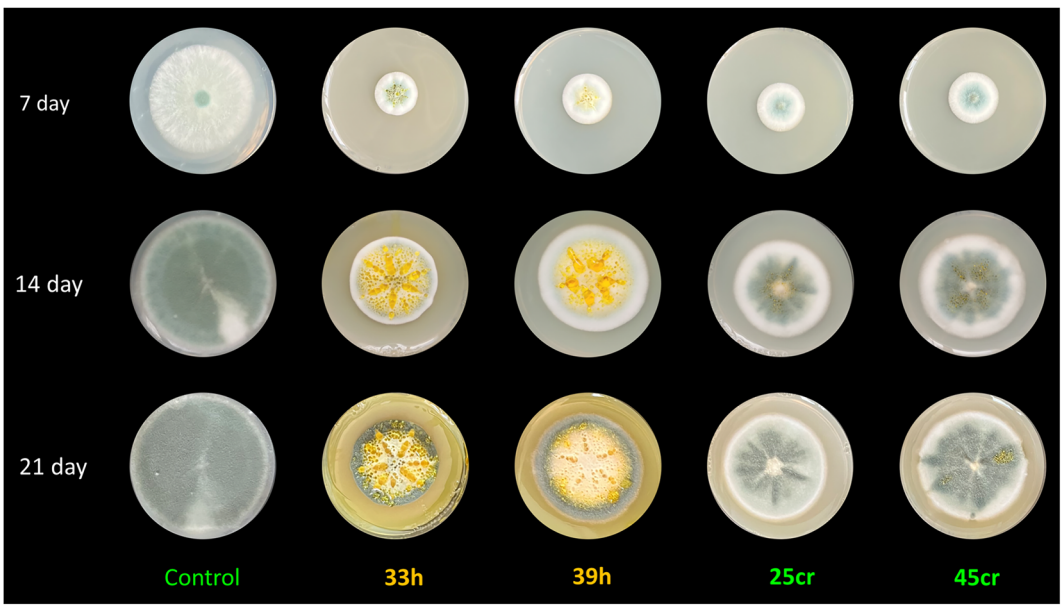

Fig. 8 Pigmentary phenotype of *Penicillium chrysogenum* STG-117 after cultivation for 7, 14 and 21 days on Czapek-Dox agar (CDA) medium with the addition 1 mg/mL chitosan or without additives (control)

lowest and highest chitooligosaccharides in the samples [48]. Moreover, discrepancies may arise from variations in the chemical structure of terminal groups and acetyl-group distribution along oligochitosan chains due to differences in hydrolysis methods [48]. The effectiveness of chitosan with diverse molecular weights in inhibiting growth is also influenced by the fungal species involved [56].

The ambiguity in experimental data on the correlation between biocidal activities and physicochemical characteristics of chitosan types is primarily due to molecular heterogeneity. Therefore, it is essential to characterise

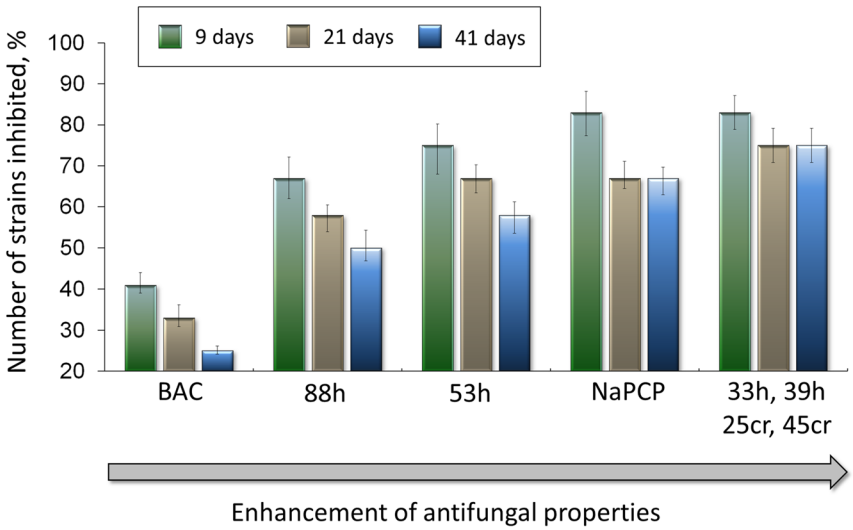

Fig. 9 The percentage of completely inhibited fungal STG microbiome (among the 12 studied strains) at 9, 21 and 41 days after inoculation

each chitosan sample by its molecular weight, degree of acetylation, and polydispersity before conducting investigations [57].

Existing literature highlights the antimicrobial properties of chitosan, yet limited information is available from the exploration of chitosan derived from insects. It was shown that the activity can be influenced by the developmental stage of *H. illucens* (e.g., larvae, pupal exuviae, or dead adults), as well as the extraction method (bleached versus unbleached chitosan samples) [16]. This pattern was similarly observed in other insect species like *Periplaneta americana*, *Blattella germanica* [58], *Antheraea mylitta* [59]. The studies' findings [15, 16] were also consistent with those obtained from chitosan derived from crustaceans, affirming that chitosan sourced from insects, particularly *H. illucens*, stands as a viable alternative to commercial chitosan for antimicrobial activity.

Conclusions

Preserving cultural heritage is paramount, and in light of the challenges posed by biodegradation, the quest for novel, eco-friendly antiseptics becomes imperative to ensure the lasting protection of our cultural treasures. Amid the growing focus on green technologies sustainable development goals, bioconverter insect farms are gaining widespread adoption. Notably, *H. illucens* seamlessly integrates into a zero-waste circular economy framework for efficient organic waste management. In our research, we utilised *H. illucens* larvae, the unpigmented source, for chitosan extraction.

Our investigation reveals that chitosan obtained from *H. illucens*, with molecular weights ranging from 33 to 88 kDa, displays inhibitory efficiency against fungi-destructors. This chitosan, alongside crab chitosan, exhibits potential as a protective material for cultural heritage sites demonstrating similar protective properties against fungi-destructors affecting painting materials.

The relationship between chitosan molecular weight and inhibition efficiency likely follows a parabolic trend within the low molecular weight range (25 to 88 kDa) achieved through chemical hydrolysis. The peak inhibition levels are observed between 25 and 45 kDa. The variation in optimal inhibition values for different fungal strains within 25–88 kDa range contributes to a blurred overall maximum, particularly within the 25–45 kDa interval.

In this context, achieving a potent inhibitor with a broad spectrum of activity is best accomplished through a blend of different chitosans. Our investigation specifically delved into chitosans from *H. illucens* with molecular weights of 33 and 39 kDa, identifying them as potent constituents for this effective inhibitor.

Acknowledgements

The authors declare no conflict of interest. No ethical approval required. No informed consent required. This research did not receive any specific grant from funding agencies in the public, commercial, or not-for-profit sectors.

Author contributions

AE—conceptualization, methodology, resources, visualization, writing—original draft, writing—review and editing. DA—methodology, resources, visualization, writing—review and editing. AK—conceptualization, methodology, visualization, resources, writing—original draft, writing—review and editing. SA—conceptualization, methodology, resources. TK—resources. AL—methodology, resources. KS—methodology, visualization, writing—original draft. NS—methodology, visualization, writing—original draft. MS—resources. VV—project administration. AZ—conceptualization, methodology, resources, visualization, writing—original draft, project administration, supervision, writing—review and editing. All authors reviewed the manuscript.

Data availability
No datasets were generated or analysed during the current study.

Declarations

Competing interests
The authors declare that they have no known competing financial interests or personal relationships that could have appeared to influence the work reported in this paper.

Author details
[1]Research Centre of Biotechnology of the Russian Academy of Sciences, Leninsky Prospect, 33, Build. 2, 119071 Moscow, Russia. [2]State Tretyakov Gallery, Lavrushinskii Peryulok, 10, 109017 Moscow, Russia. [3]Kurnakov Institute of General and Inorganic Chemistry of the Russian Academy of Sciences, Leninsky Prospect, 31, 119071 Moscow, Russia.

Received: 11 July 2024 Accepted: 9 September 2024
Published online: 17 September 2024

References

1. Gadd GM, Fomina M, Pinzari F. Fungal biodeterioration and preservation of cultural heritage, artwork, and historical artifacts: extremophily and adaptation. Microbiol Mol Biol Rev. 2024. https://doi.org/10.1128/mmbr.00200-22.
2. Salvador C, Sandu I, Sandbakken E, Candeias A, Caldeira AT. Biodeterioration in art: a case study of Munch's paintings. Eur Phys J Plus. 2022;137:1–19.
3. Tiano P. Biodegradation of cultural heritage: decay mechanisms and control methods. 2009.
4. Zhgun A, Avdanina D, Shumikhin K, Simonenko N, Lyubavskaya E, Volkov I, et al. Detection of potential biodeterioration risks for tempera painting in 16th century exhibits from State Tretyakov Gallery. PLoS ONE. 2020;15:e0230591.
5. Blair DM. Dangers in using and handling sodium pentachlorophenate as a molluscicide. Bull World Health Organ. 1961;25:597.
6. Ciferri O. Microbial degradation of paintings. Appl Environ Microbiol. 1999;65:879–85.
7. Gordon D. How dangerous is pentachlorphenol? Med J Aust. 1956;43:485–8.
8. Menon JA. Tropical hazards associated with the use of pentachlorophenol. Br Med J. 1958;1:1156–8.
9. Caruso MR, D'Agostino G, Milioto S, Cavallaro G, Lazzara G. A review on biopolymer-based treatments for consolidation and surface protection of cultural heritage materials. J Mater Sci. 2023;58:12954–75.
10. Lisuzzo L, Cavallaro G, Lazzara G, Milioto S. Supramolecular systems based on chitosan and chemically functionalized nanocelluloses as protective and reinforcing fillers of paper structure. Carbohydr Polym Technol Appl. 2023;6:100380.
11 Wang J, Pan Z, Kaczorowska MA, Bożejewicz D. The application of chitosan-based adsorbents for the removal of hazardous pollutants from aqueous solutions—a review. Sustainability. 2024;16:2615.
12. Caruso MR, D'Agostino G, Wasserbauer J, Šiler P, Cavallaro G, Milioto S, et al. Filling of chitosan film with wax/halloysite microparticles for absorption of hydrocarbon vapors. Adv Sustain Syst. 2024;8:2400026.
13. Ma J, Faqir Y, Tan C, Khaliq G. Terrestrial insects as a promising source of chitosan and recent developments in its application for various industries. Food Chem. 2022;373:131407.
14. Marques A, Nunes ML, Moore SK, Strom MS. Climate change and seafood safety: human health implications. Food Res Int. 2010;43:1766–79.
15. Khayrova A, Lopatin S, Shagdarova B, Sinitsyna O, Sinitsyn A, Varlamov V. Evaluation of antibacterial and antifungal properties of low molecular weight chitosan extracted from *Hermetia illucens* relative to crab chitosan. Mol. 2022;27:577.
16. Guarnieri A, Triunfo M, Scieuzo C, Ianniciello D, Tafi E, Hahn T, Zibek S, et al. Antimicrobial properties of chitosan from different developmental stages of the bioconverter insect *Hermetia illucens*. Sci Rep. 2022;12:1–13.
17. Lagat MK, Were S, Ndwigah F, Kemboi VJ, Kipkoech C, Tanga CM. Antimicrobial activity of chemically and biologically treated chitosan prepared from black soldier fly (*Hermetia illucens*) pupal shell waste. Microorganisms. 2021;9:2417.
18. Kemboi VJ, Kipkoech C, Njire M, Were S, Lagat MK, Ndwiga F, et al. Biocontrol potential of chitin and chitosan extracted from black soldier fly pupal exuviae against bacterial wilt of tomato. Microorganisms. 2022;10:165.
19. Aranaz I, Mengibar M, Harris R, Panos I, Miralles B, Acosta N, et al. Functional characterization of chitin and chitosan. Curr Chem Biol. 2009;3:203–30.
20. Mao S, Shuai X, Unger F, Simon M, Bi D, Kissel T. The depolymerization of chitosan: effects on physicochemical and biological properties. Int J Pharm. 2004;281:45–54.
21 Pandit A, Deshpande C, Patil S, Jain R, Dandekar P. Mechanistic insights into controlled depolymerization of chitosan using H-Mordenite. Carbohydr Polym. 2020;230:115600.
22. Tømmeraas K, Vårum KM, Christensen BE, Smidsrød O. Preparation and characterisation of oligosaccharides produced by nitrous acid depolymerisation of chitosans. Carbohydr Res. 2001;333:137–44.
23. Zhgun AA, Avdanina DA, Shagdarova BT, Troyan EV, Nuraeva GK, Potapov MP, et al. Search for efficient chitosan-based fungicides to protect the 15th-16th centuries tempera painting in exhibits from the State Tretyakov Gallery. Microbiology. 2020;89:750–5.
24 Khayrova A, Lopatin S, Varlamov V, Nardiello M, Scieuzo C, Salvia R, et al. Obtaining and study of physicochemical properties of chitin/chitosan-melanin complexes from *Hermetia illucens*. J Phys Conf Ser. 2021;1942:012003. https://doi.org/10.1088/1742-6596/1942/1/012003.
25 Khairova AS, Lopatin SA, Varlamov VP, Bogdanova SA, Shigabieva YA, Knyazev AA. Chitosan-melanin polymer complex: a promising ingredient in emulsion compositions. Polym Sci Ser D. 2022;15:295–9. https://doi.org/10.1134/S1995421222020071.
26. Khayrova AS, Sazhnev NA, Korobovskaya DV, Lopatin SA, Kildeeva NR, Varlamov VP. Isolation of chitosan-melanin complex from black soldier fly adults and obtaining nanofibrous materials based on it. Appl Biochem Microbiol. 2024;60:201–6.
27. Shagdarova BT, Lopatin SA, Konovalova MV, Ilyina V, Albulov AI, Varlamov VPP. 2016 Russian Patent No. 2627870.
28. Lyalina T, Zubareva A, Lopatin S, Zubov V, Sizova S, Svirshchevskaya E. Correlation analysis of chitosan physicochemical parameters determined by different methods. Org Med Chem Int J. 2017;1:555562.
29. Lopatin SA, Derbeneva MS, Kulikov SN, Varlamov VP, Shpigun OA. Fractionation of chitosan by ultrafiltration. J Anal Chem. 2009;64:648–51.
30. Zhgun A, Avdanina D, Shagdarova B, Nuraeva G, Shumikhin K, Zhuikova Y, et al. The application of chitosan for protection of cultural heritage objects of the 15–16th centuries in the State Tretyakov Gallery. Materials. 2022;15:7773.
31 Dumina MV, Zhgun AA, Domracheva AG, Novak MI, El'darov MA. Chromosomal polymorphism of *Acremonium chrysogenum* strains producing cephalosporin C. Russ J Genet. 2012;48:778–84.
32. Zhgun AA, Nuraeva GK, Dumina MV, Voinova TM, Dzhavakhiya VV, Eldarov MA. 1,3-diaminopropane and spermidine upregulate lovastatin production and expression of lovastatin biosynthetic genes in *Aspergillus terreus* via LaeA regulation. Appl Biochem Microbiol. 2019;55:243–54.
33. Hyvönen MT, Keinänen TA, Nuraeva GK, Yanvarev DV, Khomutov M, Khurs EN, et al. Hydroxylamine analogue of agmatine: magic bullet for arginine decarboxylase. Biomolecules. 2020;10:406.
34. Zhgun AA, Nuraeva GK, Volkov IA. High-yielding lovastatin producer *Aspergillus terreus* shows increased resistance to inhibitors of polyamine biosynthesis. Appl Sci. 2020;10:8290.
35 Hackman RH. Chemistry of insect cuticle. III. Hardening and darkening of the cuticle. Biochem J. 1953;54:371–7.
36. Peng TH, Wei LK, Chiang ECW, Yoon MSO. Antibacterial properties of chitosan isolated from the black soldier fly, *Hermetia illucens*. Sains Malaysiana. 2022;51:3923–35.
37. Lee YH, Kim SC, Nam KD, Kim TH, Jung BO, Park YI, et al. Chitosan isolated from black soldier flies *Hermetia illucens*: structure and enzymatic hydrolysis. Process Biochem. 2022;118:171–81.
38. Zhgun AA, Potapov MP, Avdanina DA, Karpova NV, Yaderets VV, Dzhavakhiya VV, et al. Biotransformation of androstenedione by filamentous fungi isolated from cultural heritage sites in the State Tretyakov Gallery. Biology. 2022;11:883.

39. Alexandrova LA, Jasko MV, Negrya SD, Solyev PN, Shevchenko OV, Solodinin AP, et al. Discovery of novel N4-alkylcytidines as promising antimicrobial agents. Eur J Med Chem. 2021;215:113212.
40. Alexandrova LA, Shevchenko OV, Jasko MV, Solyev PN, Karpenko IL, Negrya SD, et al. 3′-Amino modifications enhance the antifungal properties of N4-alkyl-5-methylcytidines for potential biocides. New J Chem. 2022;46:5614–26.
41 Makarov DA, Negrya SD, Jasko MV, Karpenko IL, Solyev PN, Chekhov VO, et al. 5-substituted uridines with activity against gram-positive bacteria. ChemMedChem. 2023;18: e202300366.
42. Zhgun AA, Eldarov MA. Polyamines upregulate cephalosporin C production and expression of β-lactam biosynthetic genes in high-yielding *Acremonium chrysogenum* strain. Mol. 2021;26:6636.
43. El Ghaouth A, Arul J, Asselin A, Benhamou N. Antifungal activity of chitosan on post-harvest pathogens: induction of morphological and cytological alterations in *Rhizopus stolonifer*. Mycol Res. 1992;96:769–79.
44. Palma-Guerrero J, Lopez-Jimenez JA, Pérez-Berná AJ, Huang IC, Jansson HB, Salinas J, et al. Membrane fluidity determines sensitivity of filamentous fungi to chitosan. Mol Microbiol. 2010;75:1021–32.
45. Hua C, Li Y, Wang X, Kai K, Su M, Shi W, et al. The effect of low and high molecular weight chitosan on the control of gray mold (*Botrytis cinerea*) on kiwifruit and host response. Sci Hortic. 2019;246:700–9.
46. Wang L, Wu H, Qin G, Meng X. Chitosan disrupts *Penicillium expansum* and controls postharvest blue mold of jujube fruit. Food Control. 2014;41:56–62.
47. Xing K, Xing Y, Liu Y, Zhang Y, Shen X, Li X, et al. Fungicidal effect of chitosan via inducing membrane disturbance against *Ceratocystis fimbriata*. Carbohydr Polym. 2018;192:95–103.
48. Kulikov SN, Lisovskaya SA, Zelenikhin PV, Bezrodnykh EA, Shakirova DR, Blagodatskikh IV, et al. Antifungal activity of oligochitosans (short chain chitosans) against some *Candida* species and clinical isolates of *Candida albicans*: molecular weight-activity relationship. Eur J Med Chem. 2014;74:169–78.
49 Sheng Z, Guo A, Wang J, Chen X. Preparation, physicochemical properties and antimicrobial activity of chitosan from fly pupae. Heliyon. 2022;8: e11168.
50. Garcia LGS, de Melo Guedes GM, Fonseca XMQC, Pereira-Neto WA, Castelo-Branco DSCM, Sidrim JJC, et al. Antifungal activity of different molecular weight chitosans against planktonic cells and biofilm of *Sporothrix brasiliensis*. Int J Biol Macromol. 2020;143:341–8.
51. Guo Z, Xing R, Liu S, Zhong Z, Ji X, Wang L, et al. The influence of molecular weight of quaternized chitosan on antifungal activity. Carbohydr Polym. 2008;71:694–7.
52. Garcia LGS, de Guedes GMM, da Silva MLQ, Castelo-Branco DSCM, Sidrim JJC, de Cordeiro RA, et al. Effect of the molecular weight of chitosan on its antifungal activity against *Candida* spp. in planktonic cells and biofilm. Carbohydr Polym. 2018;195:662–9.
53. Li R, Zhu L, Liu D, Wang W, Zhang C, Jiao S, et al. High molecular weight chitosan oligosaccharide exhibited antifungal activity by misleading cell wall organization via targeting PHR transglucosidases. Carbohydr Polym. 2022;285:119253.
54. Hernández-Lauzardo AN, Bautista-Baños S, Velázquez-del Valle MG, Méndez-Montealvo MG, Sánchez-Rivera MM, Bello-Pérez LA. Antifungal effects of chitosan with different molecular weights on in vitro development of *Rhizopus stolonifer* (Ehrenb.:Fr.) Vuill. Carbohydr Polym. 2008;73:541–7.
55. Qin C, Li H, Xiao Q, Liu Y, Zhu J, Du Y. Water-solubility of chitosan and its antimicrobial activity. Carbohydr Polym. 2006;63:367–74.
56. Younes I, Sellimi S, Rinaudo M, Jellouli K, Nasri M. Influence of acetylation degree and molecular weight of homogeneous chitosans on antibacterial and antifungal activities. Int J Food Microbiol. 2014;185:57–63.
57. Kulikov S, Tikhonov V, Blagodatskikh I, Bezrodnykh E, Lopatin S, Khairullin R, et al. Molecular weight and pH aspects of the efficacy of oligochitosan against methicillin-resistant *Staphylococcus aureus* (MRSA). Carbohydr Polym. 2012;87:545–50.
58. Basseri H, Bakhtiyari R, Hashemi SJ, Baniardelani M, Shahraki H, Hosainpour L. Antibacterial/antifungal activity of extracted chitosan from American cockroach (Dictyoptera: Blattidae) and German cockroach (Blattodea: Blattellidae). J Med Entomol. 2019;56:1208–14.
59. Jena K, Ananta S, Akthar J, Patnaik A, Das S, Singh J, et al. Physical, biochemical and antimicrobial characterization of chitosan prepared from tasar silkworm pupae waste. Environ Technol Innov. 2023;31:103200.

Publisher's Note